

High-resolution studies on laser-induced collisional-energy-transfer profiles

C. Brechignac and Ph. Cahuzac

Laboratoire Aimé Cotton, Centre National de la Recherche Scientifique II, Bâtiment 505, 91405-Orsay, France

P. E. Toschek

Institut für Angewandte Physik der Universität, D 6900 Heidelberg, West Germany

(Received 14 June 1979)

High-resolution spectra of laser-induced collisional energy transfer between europium and strontium are obtained for collisional interactions which are dipole-dipole in nature. A universal profile is found for this laser-induced excitation. For the first time a precise comparison with available calculations is possible. The line core agrees well with a theory assuming a dipole-dipole coupling, but the quasistatic wing deviates from the asymptotic behavior expected for a pure dipole-dipole interaction.

I. INTRODUCTION

During the last few years experimental and theoretical work has been devoted to studies of laser-induced collisional energy transfer (LICET) in binary mixtures of vapors.¹⁻¹⁰ In such a process the interaction between the two atomic species occurs in a strong electromagnetic field and both the collisional interaction and the photon absorption are simultaneous. This process is described by the equation

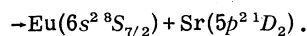
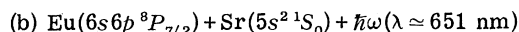
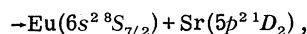
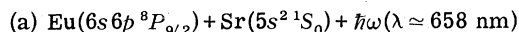
$$A|i\rangle + B|i\rangle + \hbar\omega = A|f\rangle + B|f\rangle, \quad (1)$$

where $|i\rangle$ and $|f\rangle$ are the initial and final states of the interacting species. It can be viewed as a process in which the atom B is driven at a frequency corresponding to the sum of the energies supplied by the interaction and the external field [Fig. 1(a)]. Another point of view is to consider the LICET process as a phototransition in the transient molecule (A, B) which exists during the interaction [Fig. 1(b)]. In any case excitation cannot occur without the interaction. The frequency of the external field is resonant or quasiresonant with the frequency of the interatomic transition $A|i\rangle \rightarrow B|f\rangle$, i.e., far from those characteristics of each of the interacting partners.

The efficiency of reaction (1) is characterized by a cross section $\sigma(\omega, I)$ which is proportional to the population of the $B|f\rangle$ level resulting from the induced transfer and depends on the laser frequency and on the laser flux density I . In the case of a strong laser field, its absolute value can be large compared with the kinetic cross section, and the LICET process can be applied to shift some stored energy from $A|i\rangle$ to $B|f\rangle$ in a short time. On the other hand, in the weak-field limit, $\sigma(\omega, I)$ is proportional to I and the dependence of σ vs ω , the LICET spectrum, is closely connected to the nature of the interaction between colliding partners. An analysis of the spectral profile $\sigma(\omega)$

is therefore useful for collisional studies. Specifically it gives rise to information about the interaction potential curves. It is the aim of this paper to point out such a possibility by studying the shape of the LICET spectrum.

The only spectra that have been reported to date which demonstrate the laser-induced collision^{2,3,5} do not have high enough resolution to allow for a meaningful comparison with theory. We report here the first high-resolution study of LICET spectra in a mixture of europium and strontium. Pure LICET spectra, whose resolution was not limited by the laser bandwidth, have been obtained for the following reactions:



These processes are dominated by the dipole-dipole collisional interaction. We have compared experimental profiles with spectra which were calculated by using either the traditional small-signal method which is used for the determination of collisionally broadened line shapes⁸ or by numerical integration of the coupled equations of motion.⁷

II. EXPERIMENT

The relevant levels of the system are shown in Fig. 2. The main feature is the presence of the resonant strontium level in the vicinity of the resonant europium levels. The energy defect Δ is small. The dominant interaction takes place between the $\text{Eu}(6s6p^8P_J)$ and $\text{Sr}(5p^2^1P_1)$ levels and is a dipole-dipole one. Nevertheless Δ is large enough to distinguish between the LICET process and the two-step process $\text{Eu}(6s6p^8P_J) + \text{Sr}(5s^2^1S_0) \rightarrow \text{Eu}(6s^2^8S_{7/2}) + \text{Sr}(5p^1P_1)$ followed by the resonant

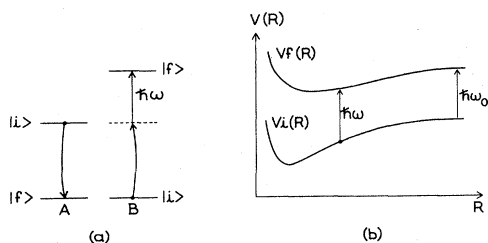


FIG. 1. Atomic and molecular pictures of the LICET process. In the first case during the interaction the atom B is driven to a virtual level and simultaneously the absorption of the photon preserves the energy balance [case (a)]. In the second case the process is a phototransition in the molecule (A, B) at a frequency ω depending on the internuclear distance R .

excitation $\text{Sr}(5p^1P_1) + \hbar\omega (\lambda = 655.0 \text{ nm}) \rightarrow \text{Sr}(5p^2^1D_2)$. This latter mechanism occurs 27\AA shifted from the LICET one in the case of the reaction (a).

The initial state $\text{Eu}(6s6p^8P_j) + \text{Sr}(5s^2^1S_0)$ with $J = \frac{9}{2}$ or $\frac{7}{2}$ is prepared by irradiation of the vapor with the light of a pulsed dye laser whose frequency is on resonance with the europium line at $\lambda = 494.5$ or 462.7 nm (coumarin 460 domain). The transfer is induced by interaction with the light of another pulsed dye laser oscillating close to the frequency corresponding to the interatomic transition $\text{Eu}(6s6p^8P_j) \rightarrow \text{Sr}(5p^2^1D_2)$ at $\lambda = 657.7$ or 651.0 nm (rhodamine 640 domain). Both dye lasers are excited with the same pulsed nitrogen laser, as is indicated in Fig. 3. The Hansch-type laser cavities¹¹ provide without Fabry-Perot etalon 4-nsec laser pulses with 5-kW peak power and a spectral width $\delta\sigma_L \approx 0.2 \text{ cm}^{-1}$. Both laser beams propagate coaxially and are focused into the active medium contained in a heat-pipe-type oven. It provides the binary mixture of europium and

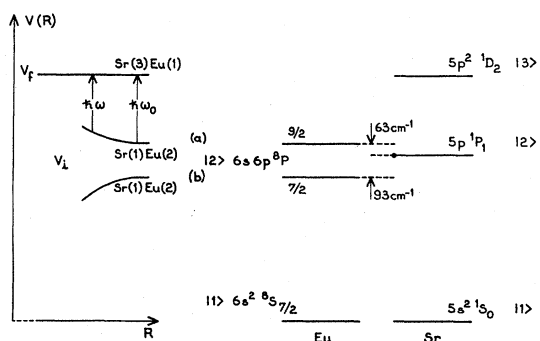


FIG. 2. Relevant levels in europium-strontium mixture (right-hand side). Corresponding representation of laser collision process in terms of a quasimolecule (left-hand side) assuming no interaction in the final state. Long-range part of the potential curves are considered only.

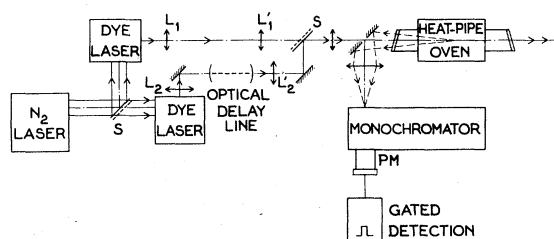


FIG. 3. Experimental setup. (L_1, L'_1) and (L_2, L'_2) are telescopic systems for the laser-beam focusing, PM the photomultiplier, and S the beam mixer.

strontium vapor and also contains a buffer gas to prevent a possible window contamination. The working temperature is around 750°C , corresponding to 0.3 and 1.2 Torr for the europium and strontium vapors, respectively. The pressure of the buffer gas, generally argon, is typically 10 Torr. The active part of the oven has a 2-cm length only. The laser flux density in the center is a few MW/cm^2 .

When the laser frequencies are adjusted for the observation of the LICET process, a large population of the final $\text{Sr}(5p^2^1D_2)$ level is achieved by direct two-photon excitation of this level. The process is efficient because of the proximity of the $\text{Sr}(5p^1P_1)$ intermediate level and hides the LICET process. In order to avoid this pure two-photon excitation in strontium, the red laser pulse is delayed relative to the blue one, by using an optical delay line (Fig. 3). We used a delay of 17 nsec, much larger than the dye-laser pulse. This delay is short compared to the effective lifetime τ of the trapped resonant europium level (typically $\tau \sim 1 \mu\text{sec}$) so that no serious lack of population occurs during this time interval.

This procedure cannot avoid a two-photon absorption to the $\text{Sr}(5p^2^1D_2)$ level where one of the photons is due to the trapped spontaneous emission from the $\text{Eu}(6s6p^8P_j)$ level. But such a possible artifact is expected to have a small probability compared with the LICET process.

The induced transfer is monitored by the observation of the fluorescence from the $\text{Sr}(5p^2^1D_2)$ level at $\lambda = 655.0 \text{ nm}$. For this purpose one observes the backward fluorescence, using a pierced mirror. A monochromator discriminates the relevant transition. This procedure avoids any diffused light due to the laser beams. For the recording a synchronous gated detection is used. The gate is coincident in time with the transfer laser pulse, whose duration is of the same order of magnitude as the fluorescence one ($\sim 20 \text{ nsec}$). High-resolution LICET spectra are obtained by recording the fluorescence intensity while the wavelength of the red laser is tuned across the

interatomic transition, which gives the cross-section profile $\sigma(\omega)$.

III. ANALYSIS OF THE EXPERIMENTAL PROFILES

A. General features

Typical LICET spectra are shown in Figs. 4 and 6. The good signal-to-noise ratio allows us to study the profile over a large detuning range ($\approx 70 \text{ cm}^{-1}$). Recordings were obtained by varying the parameters of the system, i.e., (i) the laser flux density I , from 1 to 5 MW/cm^2 , (ii) the partial pressures of europium and strontium, which were adjusted by varying the temperature in the range 700–800 °C, and (iii) the pressure of the argon buffer gas, from 5 to 20 Torr. With respect to these parameters no significant changes were observed for the line shape $\sigma(\omega)$. In particular no effects were observed due to an eventual two-photon process in strontium. We have verified that in our available laser flux-density range the absolute value of σ increases linearly with I .

The shape of the LICET spectrum is strongly asymmetrical. This is clearly understood from a molecular viewpoint: the induced transfer occurs when the laser frequency ω is smaller or larger than the interatomic frequency ω_0 , depending on the relative slope of the interaction potential curves $V_i(R)$ and $V_f(R)$ between the initial and

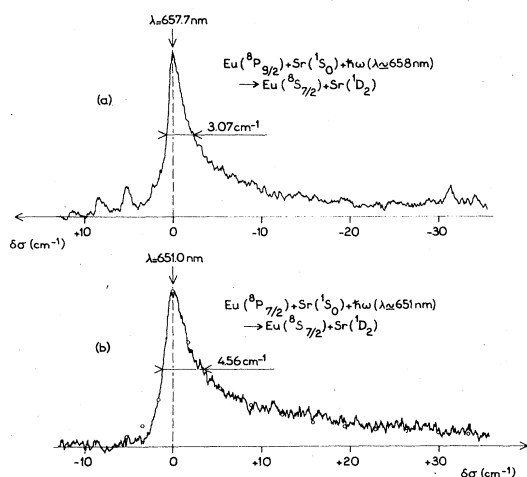


FIG. 4. Experimental line shapes when the energy is stored in the $\text{Eu}(6s6p^3P_{3/2})$, case (a), and $\text{Eu}(6s6p^3P_{7/2})$, case (b), and transferred to the $\text{Sr}(5p^2^1D_2)$ level. Notice the reversal in sign of the asymmetry between these two recordings. On curve (b) is reproduced the shape of curve (a) when their width and height are, respectively, adjusted (circles). The scale is given in wave numbers $\delta\sigma = (\omega - \omega_0)/2\pi c$.

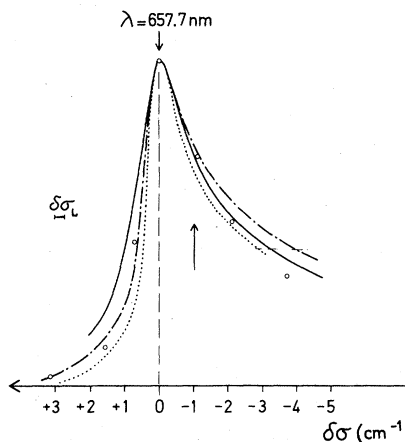


FIG. 5. Quantitative comparison of experimental line-core shape (full line) with theoretical ones [case (a) of Fig. 4]. The circle represent a numerical analysis following Harris and White⁷ for $C_6 = 3.06 \times 10^{-56} \text{ erg cm}^6$. Both dashed lines represent the calculated line-shape function $L(D, 1, U_{-1})$ as proposed by Gallagher and Holstein⁸ for $C_6 = 3.06 \times 10^{-56} \text{ erg cm}^6$ (upper curve) and $C_6 = 16.3 \times 10^{-56} \text{ erg cm}^6$ (lower curve). The arrow corresponds to a laser detuning $(\delta\sigma)_w = (1/2\pi c)/(V_0/\rho_0)$; $\delta\sigma_L$ is the laser bandwidth.

final states [Fig. 1(b)]. In addition to the LICET spectrum, sharp unidentified resonances appear under certain conditions. They are due probably to spontaneous transfer from unknown europium levels to the $\text{Sr}(5p^2^1D_2)$ level followed by a resonant light excitation. Their widths give some hint of the spectral resolution.

Within the accuracy of the measured wave numbers ($\pm 0.5 \text{ cm}^{-1}$) the signal peaks at wavelengths corresponding to the interatomic transition $\lambda = 657.7$ or 651.0 nm . This is expected in the case of a multipolar interaction between atoms and a multipole molecular moment induced by the polarization forces. In our situation the cross section increases as R^3 , where R is the internuclear separation.^{7,9}

The observed widths are always much larger than the usual Doppler or natural width, in agreement with the fact that this parameter is governed by the characteristic collision time⁸ τ_c (see the last paragraph) and not by a dephasing time (Doppler or homogeneous one).

B. Comparison of cases (a) and (b)

We have compared the experimental profiles which correspond to the reactions (a) and (b). As is also shown in a previous work,³ they exhibit an extended "quasistatic" wing, the side of which depends on the sign of the energy defect Δ . From a molecular viewpoint this result proves that for the studied reactions the dominant interaction takes place between the atomic levels $\text{Eu}(6s6p^3P_j)$ and

Sr($5p^1P_1$). Moreover, we have shown that the shapes of LICET profiles may be superimposed when their height and width are, respectively, adjusted without taking into account the sign of the energy defect Δ (Fig. 4). This result indicates that a universal profile characterizes this type of interaction. Consequently in the following we consider the interaction potential during the induced collision $\Delta V(R) = V_F - V_i(R)$, where V_F is kept constant during the collision (Fig. 2) and $V_i(R) \propto C_6 R^{-6}$, $C_6 = 4 |\mu_{12}^A \mu_{12}^B|^2 / 3\hbar\Delta$.⁷ Here μ_{12}^X is the dipole moment of the atomic transition $1 \rightarrow 2$ in atom X.

The width $\Delta\sigma(b)$ of the profile (4b) is larger than the width $\Delta\sigma(a)$ of the profile (4a). Simple calculations using the impact approximation (for details, see below) valid for the shape of the line core, use the theoretical ratio

$$\Delta\sigma(b)/\Delta\sigma(a) = \left(\frac{\Delta(b)}{\Delta(a)}\right) \times \left(\frac{\mu_{12}^A(a)}{\mu_{12}^A(b)}\right)^{1/5} = 1.13$$

derived from transition probability.¹²⁻¹⁵ The experimentally observed ratio $\Delta\sigma(b)/\Delta\sigma(a) = 1.5 \pm 0.3$ deviates from unity in the same direction as this theoretical value.

Since the shapes are identical for both cases (a) and (b) and their relative widths in agreement with a theoretical calculation, we consider in detail only the recorded profile of the reaction (a).

C. Comparison with theoretical line shape

We have compared our experimental profile with the calculated one. For this purpose we have distinguished two frequency regions: $(\omega - \omega_0)\tau_c \lesssim 1$ and $(\omega - \omega_0)\tau_c \gg 1$. The parameter τ_c is defined as the ratio between the Weisskopf radius $\rho_0 = [C_6/(\hbar V_0)]^{1/5}$ and the natural unit of velocity $V_0 = (2kT/\mu)^{1/2}$ (μ is the reduced mass): $\tau_c = \rho_0/V_0$. The line-core shape of the curve, for which $(\omega - \omega_0)\tau_c \lesssim 1$ reflects the long-range interaction. It is not very sensitive to the shape of the interaction potential, and the value of the cross section can be evaluated by using the impact approximation.⁷ In particular, at line center, an approximate formula, valid in the weak-field limit, is obtained assuming that the velocity of all atoms equals the mean relative velocity $\bar{V} = 2/\sqrt{\pi}V_0$ (Ref. 7):

$$\sigma_0 = 4\pi \left(\frac{8}{3}\right)^{2/5} \bar{V}^{-8/5} \left|\frac{C_3}{\hbar}\right|^2 \left|\frac{C_6}{\hbar}\right|^{-2/5}, \quad (2)$$

where $C_3 = \sqrt{\frac{2}{3}} [\mu_{12}^A \mu_{12}^B \mu_{23}^B / (2\hbar\Delta)] \epsilon$ (ϵ being the laser field amplitude). The line wing, for which $(\omega - \omega_0)\tau_c \gg 1$ reflects relatively short-range interactions and converges to the quasistatic limit in the neighborhood of $\omega - \omega_0 \approx V_0/\rho_0$.^{8,9} In the quasistatic approximation, both atoms are assumed to be at rest during the time interval $2\pi(\omega - \omega_0)$.

Only in this case can the LICET process be interpreted in terms of an absorption in a transient molecule. It follows that at the separation R of the atomic nuclei, absorption occurs at the frequency $\omega = \Delta V(R)/\hbar$. The LICET signal at a given detuning $\omega - \omega_0$ is due to collisions which occur at a distance $R = \{C_6/[\hbar(\omega - \omega_0)]\}^{1/6}$. This cross section in the quasistatic wing is expressed by the asymptotic law

$$\sigma(\omega) \propto R^2 \left(\frac{\partial \Delta V(R)}{\partial R}\right)^{-1} |\mu^{AB}(R)|^2, \quad (3)$$

where $\mu^{AB}(R)$ is the transition moment induced during the collision in the quasimolecule (A, B).^{8,16} In the case of a dipole-induced transition, $\mu^{AB}(R) \approx R^{-3}$, and a dipole-dipole interaction potential leads to $\sigma(\omega) \propto (\omega - \omega_0)^{-1/2}$. Taking formula (2) into account, one obtains $\sigma(\omega)/\sigma_0 = 0.757/[(\omega - \omega_0)\tau_c]^{1/2}$. This is valid for $(\omega - \omega_0)\tau_0 \gg 1$ and assuming all atoms with the velocity \bar{V} . The width at half maximum is then $\delta\sigma(\text{cm}^{-1}) = 12.1/\tau_c$.

The antistatic wing of the LICET spectrum, the abrupt fall-off side, corresponds to the no-crossing region in the dressed molecule frame. Its shape is an exponential one determined by the Massey parameter, leading in our case to $\sigma(\omega) \propto \exp\{-[(\omega - \omega_0)\tau_c]^{5/6}\}$. Actually this side of the profile might be slightly affected by the laser bandwidth $\delta\sigma_L$ and is not very useful for testing the interaction.

In Fig. 5 we compare the experimental line core with the results of two calculations. All theoretical and experimental curves are adjusted to the same peak value for the line center $\omega = \omega_0$. The first comparison is done with a universal profile deduced from the line-broadening theory of Gallagher and Holstein, in which the molecular axis rotation is ignored: $L(D, 1, U_{-1})$.⁸ Such a profile, valid in the weak-field limit, is expressed as a function of the dimensionless parameter $D = (\omega - \omega_0)\tau_c$. There is a good quantitative agreement; the "red" side of the experimental profile lies within the calculated ones for two C_6 values derived from two different sets of μ^X parameters¹²⁻¹⁵: $C_6 = 3.06 \times 10^{-56} \text{ erg cm}^6$ or $C_6 = 16.3 \times 10^{-56} \text{ erg cm}^6$. This agreement extends as far as $\omega - \omega_0 \approx 3\tau_c^{-1}$. In another attempt to calculate the line shape, we numerically integrated the equations of motion of the combined system "A + B + light field" for arbitrary laser-field amplitude ϵ . A fit to the recorded trace reveals good agreement and shows that the Van der Waals contribution ($\propto C_6 R^{-6}$) to the Eu($6s6p^3P_J$), Sr($5p^1P_1$) long-range interaction suffices for the interpretation of the line shape. The slight discrepancy in the steep wing might result, in part, from the residual laser bandwidth.

Taking into account the values of the C_6 coefficient and $V_0(750^\circ\text{C}) = 5.52 \times 10^4$ cm/sec, one deduces a reasonable mean value for the Weisskopf radius $\rho_0 \approx 26$ Å and for the characteristic collision time $\tau_c \approx 4.8$ psec. The corresponding width at half maximum for the LICET profile is then 2.53 cm^{-1} , in good agreement with the width of the "red" side of the profile. So, for the first time, calculations and experiment lead to the same value for this parameter. According to formula (2) and using the C_3 coefficient as defined in Ref. 7, one obtains for the cross section a value at the line center of $\sigma(0) \approx 500$ Å²/(MW/cm²). This value is compatible with the experimental one deduced from the measurement of the population transfer ratio $N[\text{Sr}(5p^2\ ^1D_2)]/N[\text{Eu}(6s6p\ ^3P_1)]^2$ and published in a previous work.³ Notice that this experimental determination of $\sigma(0)$ requires one to measure the absolute light power density and to take into account the trapping effect in the determination of the population transfer ratio. This is questionable and only the order of magnitude of $\sigma(0)$ is determined.

In Fig. 6 is presented a comparison between the whole recorded line profile and the theoretical one. For the line core again the result obtained from Gallagher and Holstein's model with $C_6 = 16.3 \times 10^{-56}$ erg cm⁶ is given. The quasistatic wing is expressed by the expected asymptotic law $\sigma(\omega) \propto (\omega - \omega_0)^{-1/2}$. Such an extension of the theoretical core profile is situated above the experimental curve, which varies as $(\omega - \omega_0)^{-0.85}$ as soon as $\omega - \omega_0 \approx 3\tau_c^{-1}$ (Fig. 7). According to Eq. (3) this fact indicates that terms $C_s R^{-s}$ with $s > 6$ contribute to the interaction potential. Moreover we have assumed so far that the potential V_f in the final state does not depend on R . This approximation,

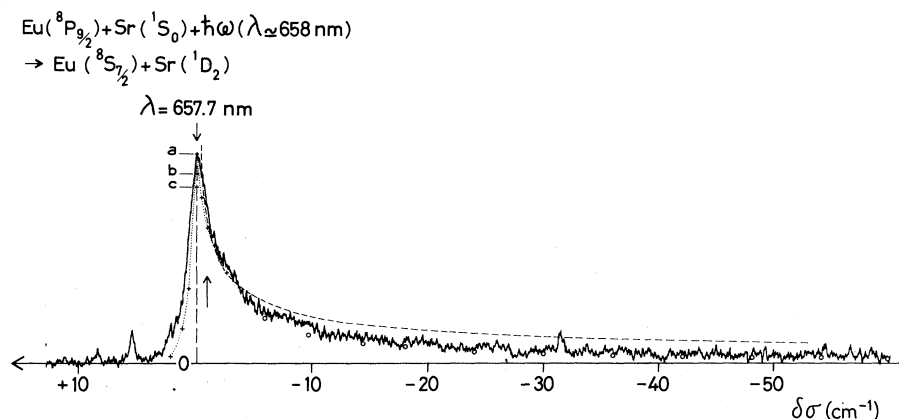


FIG. 6. Attempted fit of the whole recording. On the line core is reproduced the best fit from Fig. 5 which converges to the quasistatic limit (dashed line) at large detuning: $(\delta\sigma)^{-1/2}$. The circles represent the extension of the line core assuming a function $(\delta\sigma)^{-1}$. Points a, b, and c represent, respectively, the line-center value of the cross section: a, following Gallagher's calculation; b, the approximate C_6 theory with a \bar{V} for all atom pairs; c, the approximate C_6 theory after integration over the velocity distribution.

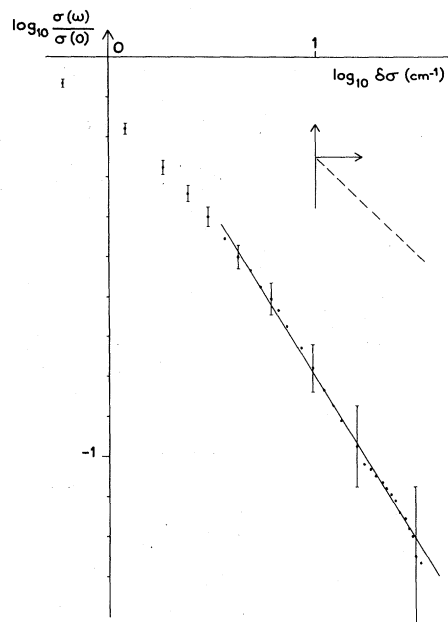


FIG. 7. Power-law dependence of the whole LICET profile. In the far wing $\sigma(\omega) \propto (\omega - \omega_0)^{-0.85}$. The theoretical slope (-0.5), expected for the dipole-dipole interaction is represented in the right-hand side (dashed line). In any case it cannot fit the experimental points.

which is valid for a long-range interaction, is probably no longer valid for collisions with smaller impact parameters. For instance, a detuning of 50 cm^{-1} corresponds to a main contribution from collisions with an impact parameter of 14 Å, a value smaller than the Weisskopf radius. In such a situation the validity of the linear-trajectories hypothesis assumed in all the calculations

are doubtful. In other words the effect of short-range interaction might be larger than is usually reported⁷ according to the area factor in the σ determination and the oscillating nature of the collision transition probability when the impact parameter is smaller than the Weisskopf radius.⁷

IV. CONCLUSION

The observed high-resolution LICET line shapes allow for the first time a quantitative comparison with line shapes calculated from first principles. For the study of atomic interaction potentials such line shapes provide us with information analogous to that derived from the shape of satellite lines connected with optical collisions. The ob-

served deviation from the expected asymptotic $(\omega - \omega_0)^{-1/2}$ dependence suggests that other case studies are of interest, in particular investigations of the dipole-quadrupole case, or of mixtures leading to bound molecules. Our results also imply that more realistic potential curves are needed for theoretical calculations.

ACKNOWLEDGMENTS

The authors wish to thank Serge Feneuille for helpful discussions during the work and Simon Roizen, Roger Leroux, and Marcel Fréville for their technical assistance. This work was supported by the Centre National de la Recherche Scientifique under A.T.P. Contract No. 3750.

¹D. B. Lidow, R. W. Falcone, J. F. Young, and S. E. Harris, Phys. Rev. Lett. 36, 462 (1976).

²R. W. Falcone, W. R. Green, J. C. White, and S. E. Harris, Phys. Rev. A 15, 1333 (1977).

³Ph. Cahuzac and P. E. Toschek, Phys. Rev. Lett. 40, 1087 (1978).

⁴W. R. Green, J. Lukasik, J. R. Willison, M. D. Wright, J. F. Young, and S. E. Harris, Phys. Rev. Lett. 42, 970 (1979).

⁵W. R. Green, M. D. Wright, J. F. Young, and S. E. Harris, Phys. Rev. Lett. 43, 120 (1979).

⁶L. I. Gudzenko and S. I. Yakovlenko, Sov. Phys. JETP 35, 877 (1972).

⁷S. E. Harris and J. C. White, IEEE J. Quantum Electron. QE13, 972 (1977).

⁸A. Gallagher and T. Holstein, Phys. Rev. A 16, 2413

(1977).

⁹S. I. Yakovlenko, Sov. J. Quantum Electron. 8, 151 (1978), and references therein.

¹⁰E. J. Robinson, J. Phys. B 12, 1451 (1979).

¹¹T. W. Hänsch, Appl. Opt. 11, 895 (1972).

¹²C. H. Corliss and W. R. Bozman, Experimental Transition Probabilities for Spectral Lines of Seventy Elements, Nat. Bur. Stand. (U.S.) Monogr. 53 (1962).

¹³V. A. Komarovski, N. P. Penkin, and L. N. Shabanova, Opt. Spectrosc. 25, 81 (1968).

¹⁴F. M. Kelly, T. H. Koh, and M. S. Mathur, Can. J. Phys. 52, 795 (1974).

¹⁵V. A. Zilitis, Opt. Spectrosc. 29, 438 (1970).

¹⁶R. E. M. Hodges, L. D. Drummond, and A. Gallagher, Phys. Rev. A 6, 1519 (1972).